High Precision 6DOF Vehicle Navigation in Urban Environments using a Low-cost Single-frequency GPS Receiver

Sheng Zhao Yiming Chen Jay A. Farrell

***Abstract*— Many advanced driver assistance systems (ADAS) demand for high precision navigation in urban environments. Traditional high precision dual-frequency RTK GPS receivers are too expensive for the low-cost, massive produced consumer-grade applications. On the other hand, many potential applications will become feasible as the high precision navigation solution becomes affordable using low-cost sensors. Hence, this paper proposed a high precision global navigation system using the low-cost single frequency GPS receiver and MEMS inertial measurement unit (IMU), with the application in GPS-challenged urban environments. By utilizing a sliding-window smoothing estimator, we are able to demonstrate reliable decimeter positioning accuracy in the presence of severe mutli-path errors and intermittent GPS signal receptions. To the best of the authors' knowledge, this is the first literature report of a high performance sliding window smoothing estimator on tightly coupled Differential-GPS/IMU using L1-only measurements in a GPS-challenged urban environment.**

I. Introduction and Related Work

High precision navigation is the core functionality in many advanced driver assistance systems, e.g. self-driving. In these systems, GPS is the primary sensor to obtain the global position of the vehicle. To achieve reliable high precision positioning, differential GPS (DGPS) is a promising approach. As the mobile communication networks (4G or WiFi) becomes ubiquitous, the DGPS technique can be used in most of the urban environments and provides 0.1 to 3 meter positioning accuracy [1].

However, GPS has its own limitations due to many factors. In the urban environments, the GPS signals can be blocked by trees and tall buildings and thus using GPS alone cannot obtain reliable and accurate navigation solutions. As an example of the poor GPS coverage in the urban environment, the satellite availability along the campus testing trajectory is shown in Fig. 1. Moreover, the traditional high-end dual frequency RTK GPS receiver is too expensive for low-cost/consumer-grade applications. In addition, in recent years, the single frequency (L1-only) GPS receivers have become readily available in the market at a much lower price than the dual frequency receiver, and the MEMS IMU is also getting much cheaper. Many potential applications will become feasible as the high precision navigation solution becomes affordable using low-cost sensors. Therefore, this paper proposes a high precision global navigation system using a low-cost single frequency GPS receiver and a MEMS IMU, with the application in GPS-challenged urban environments.

Zhao and Chen are Ph.D. students and Farrell is a Professor at the Dept. of Electrical Eng., University of California, Riverside, 92521. {shzhao, yichen, farrell}@ee.ucr.edu.

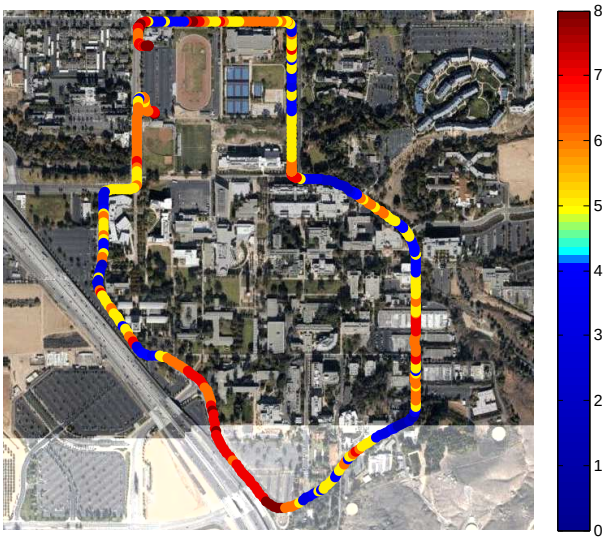

Fig. 1: The testing trajectory marked with colors to represent the number of satellites available to the receiver along the trajectory. Due to the blockage of building and trees, there are many places where less than 4 satellites can be seen (highlighted in blue color). This is a challenging route for the GPS/IMU navigation system. With the proposed method, the reliable decimeter positioning errors is achievable using L1-only GPS measurements.

In the GPS navigation community, RTK GPS positioning is a well-known mature technique. However, for low-cost, single frequency receiver, there still are many challenges, especially in urban environments. Compared to a dual frequency receiver, a single frequency receiver cannot form multi-frequency combinations which would greatly reduce the integer searching effort in realtime. Moreover, the number of measurements from single frequency receiver is half of that from a dual frequency receiver. In urban environments, the intermittent signal reception that caused by the signal blockage also creates problems because everytime the receiver reacquires the satellite signal, the integer in the carrier phase measurement is different. Therefore in practice, it is difficult or takes significantly longer for a single frequency receiver to resolve the integer and obtain the centimeter level accuracy compared to the high-end, dual frequency receivers [2]. As a result, the slow convergence rate of the positioning accuracy using a single frequency receiver is usually intolerable for many ADAS applications.

Without the correctly resolved integer, the phase measurement does not provide absolute range information. In this

case, most of the existing approaches use the triple difference technique in an EKF estimator [2], [3], [4]. However, the existing approaches either have slow convergence rate or assume perfect initialization of the estimator. In recent years, the smoothing based estimator have been demonstrated to have better performance than the EKF [5] and have been applied in many vision-aided inertial navigation systems [6], [7]. Hence, in our previous paper [8], the authors utilized a sliding-window smoothing estimator (which is named as the Contemplative RealTime (CRT) estimator) and demonstrated the superior performance to the EKF using pseudorange measurements in open sky environments. To further improve the performance of the CRT estimator in GPS-challenged urban environments, this paper proposes a novel way to utilize the accurate phase measurements in the CRT estimator when the integer cannot be resolved.

The contributions of this paper are:

1) The first literature report of a high performance sliding window smoothing estimator on tightly coupled DGPS/IMU using L1-only measurements in GPS-challenged urban environments.
2) The first literature report of utilizing the phase measurement in the sliding window smoothing estimator to achieve high precision navigation when the correct integer cannot be resolved.

II. Literature Review

For dual-frequency GPS receivers, the integer ambiguity problem is a well researched topic and there are many working solutions available [9], [10]. Once the integer is successfully resolved, an EKF is typically applied to obtain a centimeter accuracy navigation solution.

For a single-frequency GPS receiver, resolving the integer in realtime is much harder. There are many papers working on this topic by using triple difference technique, which differences the phase measurement at two consecutive times to eliminate the unknown integer. In [2], the authors designed an EKF to use the triple-difference phase measurement from a single frequency receiver to achieve submeter accuracy. The reported time needed for the estimator to converge to submeter accuracy is 500 sec and the vehicle needs to stay stationary during this period. In [3], the authors proposed an integer searching and validation method based on the technique developed in [2] with an application on a low-cost mowing robot using single frequency receivers. The time it takes to reliably resolve the integer was not reported. In [4], the authors utilize a modified triple difference technique in an EKF to track the relative positions of the receivers from a perfectly known initial configuration. The global positions are not estimated in their approach. Due to the nature of tracking (perfect initial knowledge), it does not need a long time to converge to a submeter accuracy. The reported accuracy of position tracking is in the decimeter level when the vehicle is driving in high speed.

The method proposed in this paper is related to the triple difference technique. Instead of differencing consecutive measurements to eliminate the integer, we propose a systematic way to eliminate the integer for a time window of measurements and thus creates the constraints between all the vehicle poses in the window. The proposed method is optimal in that it preserves all the information from the measurements and correctly captures the time correlation of the resulted kinematic constraints in contrast to the triple difference technique.

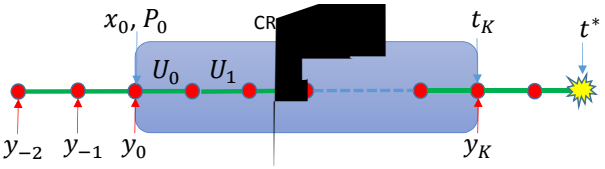

Fig. 2: The illustration of measurement time line and CRT window. The red dots represent the vehicle states at the GPS measurement time. The green lines represent the IMU constraints between two consecutive states. At t_k the optimization problem is formed and the solution of the optimization problem will be available at t^*. At t^*, the vehicle state is propagated from t_k to t^* using IMU measurements.

To fully utilize the proposed method, this paper uses a sliding window smoothing estimator. Smoothing related algorithms are getting significant attention in the SLAM community in recent years [11], [12], [6], [7]. However, none of these papers report the performance for tightly coupled DGPS/INS. The most related one is [7]. However, in that paper the GPS is integrated in a loose coupled way. Therefore, they reported similar performance between smoothing and EKF. In a tightly coupled DGPS/INS system, we notice that there is a significant performance improvement compared to the EKF, especially in GPS-challenged urban environments. The navigation system designed in this paper is similar in concept to the one proposed in [6]. However, [6] focus on the visual inertial integration and they have not reported any tightly coupled GPS/IMU results. Based on the best knowledge of the authors, we believe this is the first publication of the high performance capability of smoothing estimator on tightly coupled DGPS/INS.

III. Nonlinear Least Square Problem

This section briefly describes the optimization problem in the CRT estimator. The details of the CRT estimator can be found in [6], [8].

The measurement time line of the CRT estimator is given in Fig. 2. The IMU measurements and GPS measurements are denoted as $\mathbf{U}_k$ and $\mathbf{y}_k$ respectively. At each CRT window (a sliding window of sensor measurements), we solve a nonlinear least square problem:

$$\hat{\mathbf{X}} = \underset{\mathbf{X}}{\operatorname{argmin}} \left\{ \sum_{i \in \mathbb{S}} \|\mathbf{e}^i(\mathbf{X})\|_{\mathbf{R}^i} \right\} \tag{1}$$

where $\mathbf{X}$ is the state vector of the vehicle trajectory defined on the CRT window, the set $\mathbb{S}$ represents all the information within the CRT window which, in our case, consists of the IMU, GPS and prior information, the $\mathbf{e}^i(\mathbf{X})$ is the residual

function (IMU: $\mathbf{e}^i_\Delta$, GPS: $\mathbf{e}^i_\rho$ and $\mathbf{e}^i_\phi$, prior: $\mathbf{e}^i_0$), and $\mathbf{R}^i$ is the corresponding covariance matrix. The formulation of IMU and prior residual can be found in [8]. The GPS residuals will be discussed in the next section.

IV. Differential-GPS

DGPS has advantage over stand-alone GPS in that most of the common-mode errors (e.g., ionosphere, troposphere, satellite clock and ephemeris errors) can be removed by differencing measurements between the rover receiver and the GPS base station receiver. For simplicity of notation, it is assumed in this paper that DGPS approach completely removes all common-mode errors. Two types of measurements are provided by the receiver: pseudorange (code) and carrier phase measurements. To avoid the modeling of the receiver clock error which involves the complicated GPS measurement compensation, double differenced GPS measurements are considered in this paper.

A. Pseudorange Measurement

The double differenced pseudorange measurements for the i-th satellite vehicle (SV) can be modeled as

$$\rho^{ic} = \gamma^{ic} + mp^{ic}_\rho + n^{ic}_\rho, \tag{2}$$

where $\gamma^{ic}(t) = \bar{\gamma}^i(t) - \bar{\gamma}^c(t)$, $\rho^{ic} = \bar{\rho}^i - \bar{\rho}^c$, $n^{ic}_\rho = \bar{n}^i_\rho - \bar{n}^c_\rho$, $\bar{\gamma}^i(t) = \|\mathbf{p}_r(t) - \mathbf{p}^i_{sv}(t)\|_2$ is the geometric distance between the vehicle position $\mathbf{p}_r \in \mathbb{R}^3$ and the i-th SV position $\mathbf{p}^i_{sv} \in \mathbb{R}^3$, $\bar{\rho}^i$ is the pseudorange measurement of i-th SV, the superscript c is used to denote the common satellite chosen in the double differencing method, mp^{ic}_ρ is the multi-path error which can be several meters and $\bar{n}^i_\rho$ is the measurement noise whose standard deviation is typically around 2-5 meters.

Thus, the residual function of the double differenced code measurement can be formed from eqn. (2) as:

$$\mathbf{e}^i_\rho(\mathbf{x}(t)) = \rho^{ic} - \gamma^{ic}(t) \tag{3}$$

B. Carrier Phase Measurement

The double differenced phase measurement model for the i-th satellite vehicle (SV) is:

$$\lambda\phi^{ic} = \gamma^{ic} + \lambda N^{ic} + mp^{ic}_\phi + n^{ic}_\phi, \tag{4}$$

where $\phi^{ic} = \bar{\phi}^i - \bar{\phi}^c$ and $n^{ic}_\phi = \bar{n}^i_\phi - \bar{n}^c_\phi$, $\bar{\phi}^i$ is the phase measurement of i-th SV, N^{ic} is an unknown integer of the phase cycle, λ is the wavelength of the signal (L1 signal: 19.05cm), mp^{ic}_ϕ is the multi-path error which is in the centimeter level, and $\bar{n}^i_\phi$ is the measurement noise whose standard deviation is typically in the centimeter level. The integer N^{ic} is constant over time intervals when the receiver has phase lock for SV i and c. The receiver indicates this lock with a flag and lock time counter. Once the unknown integer N^{ic} is resolved, the phase measurement provides the range measurement in a centimeter accuracy.

However, the integer is difficult to resolve reliably in realtime for a single-frequency receiver. Nonetheless, there are at least two reasons why we still want to use the phase measurement when the integer cannot be resolved:

1) Multi-path only introduces a few centimeters of error in the phase measurement while the code measurement can be affected by few meters.
2) Phase measurements over a time window provide the local kinematic constraints of the trajectory at the centimeter accuracy even when the correct integer is not available.

Typically, there are two ways of utilizing the phase measurement when the correct integer cannot be resolved:

1) Use the triple difference technique to create an integer-free measurement. The triple difference measurement $\tilde{\boldsymbol{\phi}}^{ic}_k$ at t_k for i-th SV is defined as:

$$\lambda\tilde{\boldsymbol{\phi}}^{ic}_k = \gamma^{ic}_k - \gamma^{ic}_{k-1} + \tilde{n}^{ic}_\phi \tag{5}$$

   where $\tilde{\boldsymbol{\phi}}^{ic}_k = \phi^{ic}(t_k) - \phi^{ic}(t_{k-1})$ and $\tilde{n}^{ic}_\phi = n^{ic}_\phi(t_k) - n^{ic}_\phi(t_{k-1})$. This equation is derived by subtracting eqn. (4) at t_{k-1} and t_k. The benefit of this approach is that the resulted measurement $\tilde{\boldsymbol{\phi}}^{ic}_k$ is independent of the integer and thus it does not violate the integer assumption. However, the triple difference only consider the consecutive measurements and ignore the time correlation of phase measurements over a time window.
2) Estimate the integer as a float number together with other vehicle states in the estimator. This approach correctly accounts for the time correlation of phase measurements. The major drawback of this approach is that the integer constraint is not respected and adding integers into the estimator will increases the computational complexity.

To incorporate the accurate phase measurements in the CRT framework, this paper proposes a new method that takes benefits from both the approaches mentioned above. Furthermore, as an improvement of the triple difference technique, this paper proposes a integer-free phase measurement that is independent of the integer while correctly captures the time correlation of phase measurements. As a nutshell, the CRT estimator uses the proposed integer-free measurements for i-SV when the i-SV is not observed by the first pose in the CRT window. Otherwise the integers are added into the estimator.

V. Integer-free Phase Measurement

To fully utilize the phase measurement without resolving the integer, an integer-free measurement is constructed using methods originally proposed for visual odometry [13]. Given all the measurements of the i-th SV and the common SV c that contributes to the constant integer N^{ic}, which are defined as an integer track Ξ^{ic} in this paper, stacking up eqn. (4) and ignore the multi-path error mp^{ic}_ϕ gives:

$$\lambda\boldsymbol{\phi}^{ic} = \mathbf{h}(\mathbf{X}_{\mathbb{S}^{ic}_p}) + \lambda\mathbf{G}^{ic}N^{ic} + \mathbf{n}^{ic}_\phi \tag{6}$$

where

$$\boldsymbol{\phi}^{ic} = \begin{bmatrix} \phi^{ic}(\bar{t}_1) \\ \phi^{ic}(\bar{t}_2) \\ \vdots \\ \phi^{ic}(\bar{t}_l) \end{bmatrix}, \quad \mathbf{h}(\mathbf{X}_{\mathbb{S}_p^{ic}}) = \begin{bmatrix} \gamma^{ic}(\bar{t}_1) \\ \gamma^{ic}(\bar{t}_2) \\ \vdots \\ \gamma^{ic}(\bar{t}_l) \end{bmatrix}, \mathbf{G}^{ic} = \begin{bmatrix} 1 \\ 1 \\ \vdots \\ 1 \end{bmatrix}, \tag{7}$$

where $\mathbb{S}_p^{ic} = \{\bar{t}_1, \bar{t}_2, \ldots, \bar{t}_l\}$ denotes a set of consecutive time steps that both the i-th SV and the common SV c are observed, and $\mathbf{X}_{\mathbb{S}_p^{ic}} = \{\mathbf{x}(t) \,|\, t \in \mathbb{S}_p^{ic}\}$. The set $\mathbb{S}_p^{ic}$ always contains consecutive time steps because every time the receiver reacquires the satellite, the integer changes.

Using the methods in [13], the integer can be eliminated from the equation by the following procedure. Define a unitary matrix $\mathbf{A} = [\mathbf{A}_1, \ \mathbf{A}_2]$ such that the columns of $\mathbf{A}_2$ form the basis of the left nullspace of $\mathbf{G}$ ($\mathbf{A}_2^\top \mathbf{G} = \mathbf{0}$). Multiplying $\mathbf{A}_2^\top$ on both sides of (6) gives:

$$\lambda \bar{\boldsymbol{\phi}}^{ic} = \bar{\mathbf{h}}(\mathbf{X}_{\mathbb{S}_p^{ic}}) + \bar{\mathbf{n}}_\phi^{ic} \tag{8}$$

where $\bar{\boldsymbol{\phi}}^{ic} = \mathbf{A}_2^\top \boldsymbol{\phi}^{ic}$, $\bar{\mathbf{h}} = \mathbf{A}_2^\top \mathbf{h}$ and $\bar{\mathbf{n}}_\phi^{ic} = \mathbf{A}_2^\top \mathbf{n}_\phi^{ic}$.

Thus, the integer-free phase measurement induced residual equation $\mathbf{e}_\phi(\mathbf{X})$ can be formed as:

$$\mathbf{e}_\phi^i(\mathbf{X}) = \lambda \bar{\boldsymbol{\phi}}^{ic} - \bar{\mathbf{h}}(\mathbf{X}_{\mathbb{S}_p^{ic}}) \tag{9}$$

Note that the above derived measurement equation is independent of the integer. Equation (9) expresses the relative kinematic constraints between vehicle poses along the trajectory. The constraint is strong because the noise $\mathbf{n}_\phi^{ic}(t)$ has a standard deviation at the centimeter level. Moreover, in the proposed approach, the noise $\bar{\mathbf{n}}_\phi^{ic}$ correctly captures the time correlation of the relative kinematic constraint between all the vehicle poses in the set $\mathbb{S}_p^{ic}$ through its dense covariance matrix $\mathbf{A}_2^\top \mathbf{R}_\phi^{ic} \mathbf{A}_2$, where $\mathbf{R}_\phi^{ic}$ is the covariance matrix of $\mathbf{n}_\phi^{ic}$. In contrast, the triple difference technique only captures the pairwise kinematic constraint between two consecutive vehicle poses, but neglects time correlation between subsequent measurements.

VI. Experimental Results

This section presents analysis of data accumulated during a test drive around the campus of University of California, Riverside, see Fig. 1. Along the test path there are many trees and buildings as is representative of a typical urban environment. In the experiment, the vehicle is equipped with dual-frequency GPS receivers and a MEMS IMU, but no form of compass. For this receiver, the L1 data is more accurate than a typical low-cost single frequency GPS receiver and antenna would produce; however, using identical data is most useful for the present analysis (generating ground truth). GPS measurements are taken at 1 Hz. The GPS provides code (pseudorange) and carrier phase measurements. All GPS measurements are used in a differential mode. The IMU provides measurements at 200Hz. The CRT estimator uses 10s window of data. The vehicle position is initialized by the GPS measurement and the pitch and roll are obtained from the accelerometer assuming the vehicle is stationary. The sensor platform is shown in Fig. 3.

Fig. 3: Navigation and Mapping sensor platform. Equipped with GPS/INS unit, monocular camera, 360 degree camera, 2D LIDAR, RADAR, and Velodyne LIDAR.

The trajectory estimation error is formulated by subtracting the real-time state estimate at each time from a ground truth state estimate for the same time. The ground truth trajectory is determined by an off-line, post-processed smoother combining the IMU and integer-resolved phase measurements (using L1 and L2 measurements) [14]. The ground truth trajectory is accurate at the centimeter level. All the CRT estimators used in the experiment use L1 only measurements.

Fig. 4 shows the position, velocity and attitude errors of the CRT estimator using code and phase. As we can see from the results, the position error is within $\pm 0.5m$ for most of the time in the horizontal plane (north and east direction), the velocity error is within $\pm 0.1m/s$ and the roll and pitch errors are within $\pm 0.2^\circ$ and the yaw error is within $\pm 1^\circ$ without using a compass.

To demonstrate the benefits of phase measurements, the position errors of the CRT estimator using code only are shown in Fig. 5 with the position errors of the CRT estimator using code and phase. We can see that the phase measurements are able to provide accurate local kinematic constraints that prevent large jumps in the position estimates in the presence of multi-path errors and noisy GPS signal receptions, even when the integer cannot be resolved. Moreover, the estimated trajectory using phase measurement is in general smoother than using the code measurements only.

VII. Conclusions and Future Work

This paper has proposed a novel DGPS/IMU navigation system that significantly improves performance in urban environments. The experimental results demonstrated that the proposed method has the potential to enable the high precision navigation using low-cost, single frequency GPS receivers and MEMS IMU in GPS challenged environments.

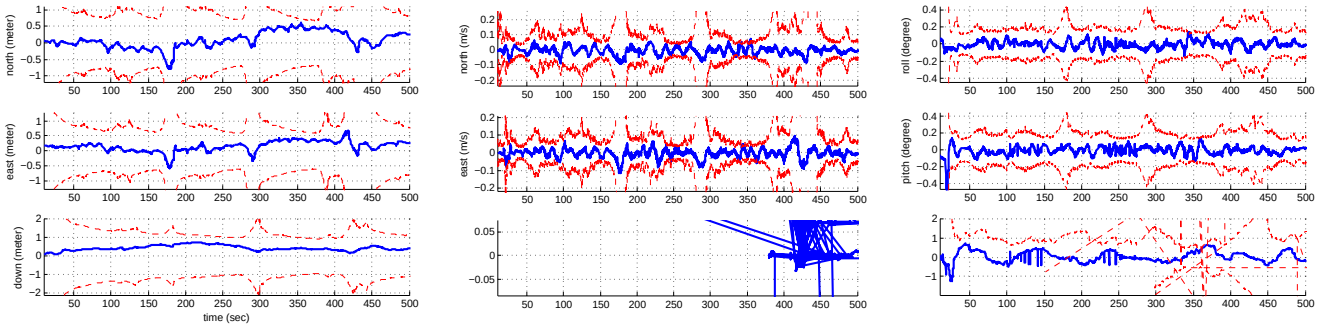

(a) Position error. (b) Velocity error. (c) Attitude error.

Fig. 4: Navigation system errors. The $\pm 3\sigma$ bound is plotted in red.

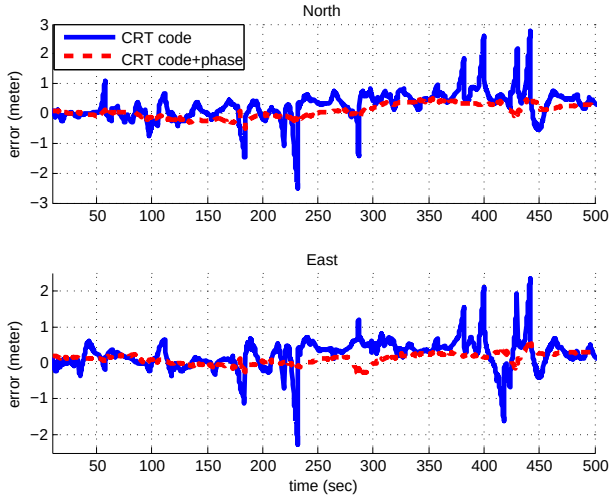

Fig. 5: North and East position errors comparison. Without using the phase measurements, the position errors have huge jumps in the presence of multi-path issues and noisy measurements when under trees.

The new algorithm performs optimization in realtime, for all IMU and GPS measurement within a time window, to provide a state estimate at the current time. The approach leads to improved performance for a few reasons. First, optimization over a time window provides the capability to re-linearize the system kinematic and measurement models around the improved trajectory estimate. This leads to the ability to estimate attitude and biases, especially yaw, accurately without a magnetometer. Second, the large set of measurement data provides sufficient redundancy to allow the effects of noise to be significantly reduced in the optimization. Third, the proposed integer-free phase measurement is able to provide accurate local kinematic constraints, without needing to resolve the integers, which helps to improve the robustness to multi-path errors and GPS noise, which are common in urban environments.

In the future, we plan to integrate the visual odometry into the existing GPS/IMU system to improve the performance. In addition, we are also working on the multi-path error modelling to correctly accounts for it.

VIII. Acknowledgements

This research builds on the software of and technical conversations with Anastasios I. Mourikis and Mingyang Li. These technical collaborations are greatly appreciated.

References

[1] J. A. Farrell, *Aided Navigation: GPS with High Rate Sensors*. McGraw Hill, 2008.

[2] J. Codol and A. Monin, "Improved triple difference GPS carrier phase for RTK-GPS positioning," in *Statistical Signal Processing Workshop (SSP), 2011 IEEE*. IEEE, 2011, pp. 61–64.

[3] J.-M. Codol, M. Poncelet, A. Monin, and M. Devy, "Safety robotic lawnmower with precise and low-cost L1-only RTK-GPS positioning," in *Proceedings of IROS Workshop on Perception and Navigation for Autonomous Vehicles in Human Environment, San Francisco, California, USA*, 2011.

[4] W. Hedgecock, M. Maroti, J. Sallai, P. Volgyesi, and A. Ledeczi, "High-accuracy differential tracking of low-cost GPS receivers," in *ACM MobiSys*, 2013.

[5] H. Strasdat, J. Montiel, and A. J. Davison, "Real-time monocular SLAM: Why filter?" in *Robotics and Automation (ICRA), 2010 IEEE International Conference on*. IEEE, 2010, pp. 2657–2664.

[6] H.-P. Chiu, S. Williams, F. Dellaert, S. Samarasekera, and R. Kumar, "Robust vision-aided navigation using sliding-window factor graphs," in *ICRA*, 2013.

[7] V. Indelman, S. Williams, M. Kaess, and F. Dellaert, "Factor graph based incremental smoothing in inertial navigation systems," in *IEEE Information Fusion (FUSION)*, 2012, pp. 2154–2161.

[8] S. Zhao, Y. Chen, H. Zhang, and J. A. Farrell, "Differential GPS aided inertial navigation: a contemplative realtime approach," in *IFAC World Congress*, 2014.

[9] T. Takasu and A. Yasuda, "Development of the low-cost RTK-GPS receiver with an open source program package rtklib," in *International Symposium on GPS/GNSS, International Convention Center Jeju, Korea*, 2009.

[10] X.-W. Chang and T. Zhou, "MILES: MATLAB package for solving mixed integer least squares problems," *GPS Solutions*, vol. 11, no. 4, pp. 289–294, 2007.

[11] F. Dellaert and M. Kaess, "Square Root SAM: Simultaneous Localization and Mapping via Square Root Information Smoothing," *Int. J. Rob. Res.*, vol. 25, no. 12, pp. 1181–1203, 2006.

[12] M. Kaess, A. Ranganathan, and F. Dellaert, "iSAM: Incremental Smoothing and Mapping," *IEEE Trans. Robotics,*, vol. 24, no. 6, pp. 1365–1378, 2008.

[13] A. Mourikis and S. Roumeliotis, "A Multi-State Constraint Kalman Filter for Vision-aided Inertial Navigation," in *IEEE ICRA*, 2007, pp. 3565–3572.

[14] A. Vu, J. Farrell, and M. Barth, "Centimeter-accuracy smoothed vehicle trajectory estimation," *Intelligent Transportation Systems Magazine, IEEE*, vol. 5, no. 4, pp. 121–135, 2013.